Results in Engineering 25 (2025) 103642

Contents lists available at ScienceDirect

Results in Engineering

journal homepage: www.sciencedirect.com/journal/results-in-engineering

Research paper

Far-UVC (222 nm) disinfection performance in residential spaces: Experimental study on *Bacillus subtilis* contamination

Jong-Il Bang [a], Ye-Lim Jo [a], Eun-Tack Lee [b], Minki Sung [a,*]

[a] Department of Architectural Engineering, Sejong University, 209 Neungdong-Ro, Gwangjin-Gu, Seoul, 05006, Republic of Korea
[b] ENG & Innovation Division, SAMSUNG C&T Corporation, Seoul, 05288, Republic of Korea

ARTICLE INFO

Keywords:
Far-UVC (222 nm)
Microbial contamination
Residential space
Disinfection
Radiation analysis

ABSTRACT

Ultraviolet germicidal irradiation (UVGI) with a 254 nm wavelength is widely used for sterilization due to its high efficacy in microbial inactivation. However, its application in daily environments is hindered by potential risks to skin and eye health upon direct exposure. Recently, far-UVC light at a safer wavelength of 222 nm has shown promise in maintaining human safety while effectively inactivating microorganisms. This study evaluates the disinfection performance of far-UVC (222 nm) in typical residential settings, specifically in high-touch areas such as shoe racks and bathrooms, with varied irradiation distances and times. Targeting *Bacillus subtilis*, a resilient model organism, we observed significant microbial reductions: a 91 % reduction on shoe racks within 5 min and a 50 % reduction in bathrooms over 4 h Calculated sterilization coefficients (*k* values) for *B. subtilis* on shoe racks and in bathrooms were 0.196 m^2/J ($R^2 = 0.98$) and 0.202 m^2/J ($R^2 = 0.81$), respectively, closely matching the manufacturer's specification of 0.1956 m^2/J. Far-UVC also demonstrated compliance with IEC 62471 safety standards, supporting its use in daily residential environments. These findings support the evidence for far-UVC's efficacy and safety in controlling microbial contamination in residential spaces, offering practical solutions for enhanced hygiene management in high-contact areas within households.

1. Introduction

The coronavirus disease 2019 (COVID-19) pandemic, which first broke out in December 2019, has resulted in approximately 700 million confirmed cases and 7 million deaths as of October 2023 [1,2]. Although previous cases of severe acute respiratory syndrome (SARS) and Middle East respiratory syndrome (MERS) occurred during the spread of infections, COVID-19 has had a more extensive and damaging impact worldwide. Consequently, substantial efforts have been made to prevent and manage the spread of the infection inside buildings. Following the spread of SARS and MERS, South Korea implemented measures to isolate infected patients by revising related standards and laws and expanding special facilities, such as negative-pressure isolation rooms for medical facilities [3]. Patient isolation was challenging with COVID-19 owing to its incubation period. Consequently, cluster infection cases occurred in various types of buildings (e.g., housing, commercial facilities, schools, offices, sports facilities, restaurants, and religious facilities) [3–8]. The South Korean government attempted to curb the spread of the infection through social regulations focusing on personal hygiene management, such as mandatory mask-wearing, hand washing, social distancing, and restrictions on commercial facilities; however, moral and religious issues hindered clear responses. Internationally, cases of infection have been reported in various buildings, and epidemiological investigations revealed diverse transmission pathways. The spread of infection in Hong Kong's Amoy Garden was attributed to external winds to the housing complex or the evaporation of beacon water in U-traps, which affected nearby buildings due to shared drainage facilities [9,10]. In addition, the spread of infection at a restaurant in Guangzhou, China, in 2020 was attributed to airflow propagation through indoor ventilation [11,12]. Even in high-rise apartment buildings, infections spread despite no direct contact, which is attributable to the stack effect among structural features [13]. An epidemiological investigation into the route of infection conducted in China for COVID-19 revealed that the spread of indoor infections occurred in various buildings, such as houses, airports,

Abbreviations: CFD, Computational fluid dynamics; CFU, Colony-forming units; COVID-19, Coronavirus disease 2019; IAQ, Indoor air quality; ID-UVGI, In-duct ultraviolet germicidal irradiation; MERS, MIDDLE East respiratory syndrome; SARS, Severe acute respiratory syndrome; TLV, Threshold limit value; TSA, Tryptic soy agar; UR-UVGI, Upper-room ultraviolet germicidal irradiation; UVGI, Ultraviolet germicidal irradiation.

* Corresponding author.
E-mail address: mksung@sejong.ac.kr (M. Sung).

https://doi.org/10.1016/j.rineng.2024.103642
Received 4 September 2024; Received in revised form 25 November 2024; Accepted 3 December 2024
Available online 6 December 2024

restaurants, and shopping malls, with approximately 80 % being home-based outbreaks [14].

Microbial damage in buildings is attributed to infectious diseases and mold damage resulting from factors such as flooding, leakage, and condensation, which pose health risks to occupants. This issue has been considered in indoor air quality (IAQ), particularly in housing facilities where people spend significant amounts of time and seek relaxation. Typical housing conditions fall within the range suitable for microbial growth. Microbes introduced from the outside or diffused indoors attach to indoor surfaces, leading to damage. This manifests as visible damage perceptible by smell or sight but can also occur in unseen places, causing building performance deterioration and health problems. Consequently, various standards and measures have been proposed for damage recovery [15–22]. They primarily include ratings according to the surface damage area and a recovery and management plan according to the scale, and they identify the degree of damage according to the indoor airborne microorganism concentration. However, the corresponding countermeasures are complicated and time-consuming. In addition, they are difficult to manage because they require professional interventions.

Various measures have been proposed to prevent the spread of infection in indoor environments based on an unspecified number of people in a general environment. Ultraviolet germicidal irradiation (UVGI) has been employed to control microorganisms on surfaces, underwater, and in the air, using chemical reactions to sterilize microorganisms. Of note, the sterilization effect is the highest near a wavelength of approximately 260 nm [23,24]. This wavelength inactivates the structure of nucleic acids and proteins in microbial cells by damaging them through photochemical changes, rendering DNA replication impossible. Referring to these standards [23–27], UVGI systems are typically applied to buildings as in-duct UVGI (ID-UVGI) or upper-room UVGI (UR-UVGI) to prevent the spread of infection and manage IAQ. These systems are also implemented in various fields, such as food and medicine. The performance of UVGI systems applied to buildings was verified through experiments and simulations. ID-UVGI can cause microbial damage inside air-handling units through humidification. Moreover, microorganisms can be introduced into the supplied air during the air-conditioning process, causing IAQ deterioration [28–34]. Besides, performance prediction and evaluation have been conducted according to the type of pollutant, UV output, and various environmental conditions through simulation analysis [33,35,36]. UR-UVGI is primarily applied to occupied indoor spaces, with significant impacts on the installation locations and indoor environments (ventilation). Many verification studies have been conducted through experiments and simulations, including full-scale mock-up experiments on airborne viruses and experimental investigations of special facilities, such as negative-pressure isolation rooms [37–45]. Studies have also been conducted to analyze sterilization performance and its correlation with influencing factors according to the air change rate through computational fluid dynamics (CFD) analysis [46–52].

Direct human exposure to UVGI can cause skin and eye damage, limiting its applicability. Accordingly, the threshold limit value (TLV) is presented as a safety standard for workers dealing with UV rays, and careful monitoring of UV lamps is imperative owing to the potential ozone formation. Consequently, UVGI systems applicable to general indoor environments have been developed, such as air purifiers, total heat exchangers, and air circulation devices that use UV-LED. Nevertheless, the potential harm caused by UVGI to humans still requires resolution.

In addition to safety evaluations for human exposure, verification and research on far-UVC (222 nm) radiation, with proven microbial reduction performance, have been conducted, as summarized in Table 1. In particular, safety assessments for humans in the biological field involved comparisons between UV-C (254 nm) and far-UVC (222 nm), primarily in mammals (mouse leather). The effect of microbial inactivation on the degree of DNA destruction and dose in various microorganisms was examined. Subsequent studies using 222 nm examined the effects of indoor microbial control in compliance with the 8-h exposure limit (TLV) suggested by the American Conference of Governmental Industrial Hygienists. The need to control microorganisms (infectious bacteria) in indoor spaces has been emphasized since the COVID-19 pandemic. The effects of the implemented control measures against the virus were also reviewed. Before the COVID-19 pandemic, safety evaluation primarily involved DNA damage evaluation using bacteria and mice, comparing far-UVC with the existing UV-C (254 nm). Far-UVC spans wavelengths of up to 200–220 nm, with high dosage requirements for an effective control effect [53–55] confirmed through daily experiments with a fixed dose [56,57]. The effect of disinfection on viruses has also been examined [58]. Following COVID-19, the controlling effects of far-UVC against various microorganisms and SARS-CoV-2 have also been evaluated [59–61]. Its effectiveness against airborne and surface microorganisms has also been confirmed [62,63]. In addition, the performance at 222 nm was demonstrated using various indicators, such as equivalent air change per hour, reduction rate, and RT-qPCR [64,65]. Despite its effectiveness in controlling microorganisms, its validation through field experiments remains limited.

UVGI has been widely studied and implemented to control microorganisms in healthcare, commercial, and laboratory environments.

Table 1
Previous research on environmental factors.

Ref.	Year	Microorganisms	Setup	Evaluation
53	2013	*MRSA, human cell (AG1522)*	207 nm, Air	$D_{99.99} = 135$ mJ/cm^2 for MRSA compared 254 nm
54	2016	Mice skin	207 nm	DNA damage (for safety) compared 254 nm
55	2017	Mice skin	222 nm (41 cm, 7 h)	DNA damage (for safety) $D = 157$ mJ/cm^2
56	2018	Mice skin	222 nm (450 mJ/cm^2/day)	DNA damage (for safety) during 1,2,3,4,5,8,9,10 days
57	2018	*MRSA* Mice skin	222 nm (5 mW/cm^2 at 1 cm)	DNA damage (for safety) during 3,5,8,12 days compared 254 nm
58	2018	*Influenza A (H 1N1)*	222 nm ($D = 0$, 0.8, 1.3, 2.0 mJ/cm^2)	$k = 1.8$ cm^2/mJ $D_{95} = 1.6$ mJ/cm^2
59	2020	*HCoV-229E HCoV-OC43 Influenza A (H 1N1)*	222 nm, Air	D_{90} (mJ/cm^2), k (cm^2/mJ) 0.56, 4.1 for HCoV-229E 0.39, 5.9 for HCoV-OC43 1.3, 1.8 for Influenza A (H 1N1)
60	2020	Mice skin	222 nm (1 mW/cm^2 at 30 cm)	DNA (for safety)
61	2020	*B. subtilis B. cereus B. thuringiensis S. aureus C. difficile Herpes virus*	222 nm, Surface	DNA damage (for safety)
62	2021	*SARS-CoV-2*	222 nm, Surface (0.1 mW/cm^2 at 24 cm)	$TCID_{50}$, RT-qPCR 99.7 % reduction for 30 s (based $TCID_{50}$)
63	2022	*B. subtilis E. coli P. chrysogenum C. cladosporidides*	275, 370, 385, 405 nm (15 cm)	k value by wavelength Reduction rate
64	2022	*MRSA HCoV-229E HCoV-OC43 H 1N1*	222 nm, Air lamp	8-h dose eACH Reduction rate
65	2022	*SARS-CoV-2*	222 nm, Water (solution)	RT-qPCR, $D_{90} = 1.6$ mJ/cm^2, $k = 0.64$ cm^2/mJ
66	2022	*E. coli ESBL S. faecalis MRSA H 1N1 H3N2 C. albicans*	Laboratory Lift cabin (surface, air) according to dose (30 cm)	Confirmed disinfection Surface 5.2 mJ/cm^2 Air 15 mJ/cm^2

Conventional UV-C at 254 nm has been shown to effectively inactivate microorganisms by damaging their DNA and RNA structures, preventing replication, and ensuring sterilization. However, direct human exposure to this wavelength poses significant health risks, limiting its application in occupied environments. To address this limitation, far-UVC (222 nm) has emerged as a promising alternative. Unlike traditional UV-C, far-UVC does not penetrate the outer layers of human skin or eyes, making it safer for use in spaces where people are present. Many studies have demonstrated its efficacy in inactivating various pathogens, including airborne and surface microorganisms while maintaining compliance with established safety standards for human exposure. For instance, studies have examined far-UVC's microbial reduction performance using metrics such as equivalent air changes per hour, reduction rates, and RT-qPCR analysis, confirming its effectiveness against viruses like SARS-CoV-2 and other pathogens [53–65].

Many microbial control effects and safety evaluations of far-UVC (222 nm) have been conducted. However, verification through field applications is necessary. Although the performance verification of microorganisms and handles (surface) in the air has been conducted in a full-scale lift cabin [66], extending this validation to residential spaces is imperative. Additionally, comparing the results with the spectral data suggested by the 222 nm module manufacturer is crucial. An actual indoor space has many environmental variables, such as reflections and airflow. Thus, it is necessary to review the performance of far-UVC (222 nm) radiation in indoor spaces. Residential spaces, however, present unique challenges for disinfection. These environments are dynamic, with varying environmental conditions and high-contact surfaces frequently exposed to microbial contaminants introduced through daily activities.

Previous studies in environmental engineering and sustainability have investigated the complex interactions between environmental factors and contaminant behavior. For example, the transport of contaminants through porous media under groundwater flow highlights how the physical and chemical properties of the environment affect contaminant persistence [67–69]. Other researchers have analyzed how moisture levels and material properties influence pollutant reduction, emphasizing the importance of environmental variables in sustainability contexts [70–72]. Studies on composite materials under varying environmental conditions further illustrate how material-environment interactions can impact contaminant behavior [73–75]. These findings underscore the critical role of environmental factors—such as airflow, moisture, and material composition—in determining the persistence and reduction of contaminants.

While these studies focus on broader environmental and material science processes, their findings emphasize the necessity of accounting for environmental variables when evaluating disinfection performance. This perspective is particularly relevant for residential settings, where dynamic environmental factors like ventilation, surface material properties, and microbial behavior can significantly influence the efficacy of far-UVC disinfection. By addressing these challenges, our study seeks to bridge this gap by investigating far-UVC's disinfection performance on high-contact surfaces under real-world residential conditions.

This study aims to address a critical gap in the application of far-UVC (222 nm) technology by examining its irradiation efficacy in residential environments. Unlike controlled healthcare or commercial settings, residential spaces present unique challenges, such as variable environmental conditions, diverse surface types, and frequent human interaction, which can influence microbial contamination and disinfection performance. By targeting high-contact surfaces like shoe racks and bathrooms, this study provides foundational data on far-UVC's practical application in dynamic residential conditions.

Furthermore, this research emphasizes safety and efficacy by validating disinfection performance under real-world conditions while adhering to established exposure standards. The findings aim to contribute to the broader adoption of far-UVC technology, not only as an effective disinfection method but also as a sustainable solution for improving indoor hygiene in everyday living environments. By addressing these challenges, our study bridges the gap between laboratory findings and practical implementation, offering insights that can inform future designs of far-UVC systems tailored to residential spaces.

2. Materials and methods

2.1. Experimental overview

An experiment was performed in an experimental building with a full-scale mock-up to evaluate the microbial control performance of the far-UVC (222 nm) module in a residential space. The target space was an experimental building for evaluating various environmental performances (e.g., ventilation and insulation) in residential spaces. This building was a commonly distributed apartment type with an area of approximately 140 m^2, comprising three bedrooms and two bathrooms. The experiment focused on bathrooms (toilets) selected based on the sanitary activities of the occupants in the residential space. In addition, the lower part of the shoe rack was selected, considering the presence of pollutants attached to shoes introduced from the outside.

Far-UVC (222 nm) modules were configured for the shoe racks and toilets. Lighting equipment was installed in the shoe rack and toilet, as shown in Fig. 1, to verify the reduction in performance when applying far-UVC (222 nm). The toilet was intensively irradiated by applying a down-light type to control microorganisms in human feces and urine discharge. The shoe rack was a bar type with far-UVC (222 nm) modules placed at both ends and general LEDs were applied in the middle.

2.2. Far-UVC (222 nm) module

The far-UVC (222 nm) module used in this study was a krypton-chloride (Kr-Cl) excimer lamp (Care 222, USHIO). It has been proven to be safe for humans compared to general UV-C (254 nm) rays. The intensity and wavelength were measured at 10 cm using a spectrometer (Black-Comet C-50, StellarNet, Tampa, FL, USA), as shown in Fig. 2 and Table 2. This product has been improved to enhance safety by incorporating an optical filter, has been evaluated for safety based on the IEC 62471 standards, and has received a test certificate to verify compliance. In addition, although the far-UVC (222 nm) modules use the same light source, the form of the lighting fixture differs. Therefore, although it may differ from the product specification, a performance evaluation was conducted by comparing the k value for microorganisms with the experimental results suggested by the manufacturer.

2.3. Microorganisms

This study focused on bacterial experiments to assess the efficacy of far-UVC lamps in reducing contamination. Despite initially framing the context of COVID-19 risks and mold issues, it is crucial to acknowledge

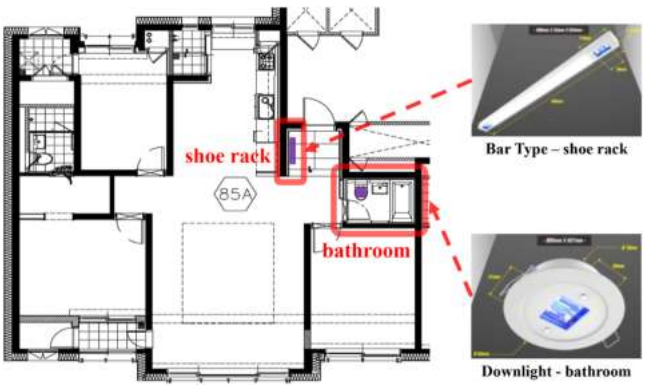

Fig. 1. Plan of target space and far-UVC (222 nm) module location.

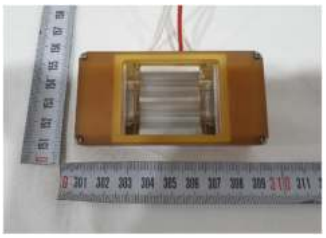

Fig. 2. Far-UVC base module.

Table 2
Specifications of far UV-C modules at 10 cm.

	222 nm
Peak wavelength (nm)	221.88
Centroid wavelength (nm)	221.54
FWHM (full width at half maximum)	3.99
Intensity (μW/cm^2)	106.4

that the experiments solely addressed bacteria, thus lacking direct relevance to virus or mold inactivation. However, recognizing that the findings could serve as a foundation for extrapolating to other pathogens, such as SARS-CoV-2 and mold, contingent upon acquiring additional data from similar experiments or models would offer a more comprehensive perspective without diminishing the significance of the results obtained.

The experiment was performed in a full-scale residential space mock-up. However, the actual infectious virus (SARS-CoV-2) was unavailable. Therefore, it was replaced with general bacteria that do not damage buildings or humans. *B. subtilis*, a nonpathogenic bacterium [75–77] primarily detected in the general environment, was obtained from the Korean Culture Center of Microorganisms (ATCC 6633) and used in the experiment. We selected *B. subtilis* for several reasons. First, it is recognized as a resilient model organism, highly resistant to environmental stress, which allows for rigorous testing of far-UVC efficacy. If far-UVC is effective against *B. subtilis*, which has higher resistance than many other microorganisms, it is likely to be effective against less-resistant species as well. Second, *B. subtilis* is widely accepted in the field as a standard model for UV disinfection studies, facilitating comparison with existing research and providing reliable, interpretable results. Lastly, as a nonpathogenic bacterium, *B. subtilis* presents minimal risk to humans and the environment, allowing safe experimental procedures without the need for high-level containment [67,78]. In addition, the far-UVC (222 nm) product specifications used in this study included experimental data on *B. subtilis*.

The appropriate dilution concentration of *B. subtilis* (ATCC 6633) was previously confirmed, and a control group was produced on tryptic soy agar (TSA) medium. A lyophilized strain of *B. subtilis* (ATCC 6633) was diluted in 9 mL NaCl (0.85 % saline) sterile solution. Consequently, the dilution concentration confirmed in the pre-experiment, undiluted (10°), 10^{-1}, and 10^{-2} times were identified as too numerous to count, with 10^{-3} and 10^{-4} times averaging approximately 1000 and 93.2 CFU/mL, respectively. An experiment with the control case diluted 10^{-3} times was performed to confirm the reduction performance of the far-UVC. The *B. subtilis* (ATCC 6633) used in the experiment was incubated for 1–2 d at 32 °C. Microorganism concentration was quantified in terms of colony-forming units (CFU) [79].

The survival rate of the microorganisms is expressed in Eq. (1) [23] and can be converted into Eq. (2).

$$Survival\ Rate = e^{-kIt} = e^{-kD} = \frac{N_t}{N_0}, \tag{1}$$

$$Killing\ Rate = 1 - e^{-kIt} = 1 - \frac{N_t}{N_0}, \tag{2}$$

$$D_{90} = -\ln(1 - 0.9)/k, \tag{3}$$

where k is the UVC sterilization coefficient (m^2/J); a characteristic of each microorganism that indicates its susceptibility to UVC; I is the UVC intensity (W/m^2); t is the UVC exposure time (s). The sterilization effect is proportional to k, I, and t; N_t is the microorganism concentration level after t (s) irradiation; N_0 is the initial concentration; and D (dose, J/m^2) is the product of I and t.

The experimental results enabled the reversal of the k value for far-UVC (222 nm) of microorganisms. In this study, the k value represents the susceptibility of microorganisms to UVC exposure, specifically quantifying the disinfection rate as a function of dose. The k value provides a measure of how effectively a particular microorganism is inactivated per unit of UV dose, with higher k values indicating greater sensitivity to UV exposure. This parameter is instrumental in comparing disinfection efficacy across different studies and ensuring the reproducibility of results under similar conditions. However, while the k value remains relatively constant for a specific microorganism under controlled conditions, it may vary when applied across different distances and surface types due to factors, such as UV intensity distribution, surface reflectivity, and environmental variables (e.g., humidity, temperature). For instance, increased distance from the UVC source reduces the intensity, requiring longer exposure times to achieve comparable microbial reduction. These variations suggest that careful calibration and consideration of environmental conditions are essential for applying k values reliably in practical settings. The product specification performance and reduction rate by irradiation time and D_{90} (mJ/cm^2), which represents the dose required to achieve 90 % disinfection of the microorganisms exposed to far-UVC, were compared by referring to the indicators used to evaluate the performance in previous studies [53,55,58,59,65].

2.4. Experimental setup

The experiment proceeded with the production of dilution solutions using solid strains, dispensing media, far-UVC (222 nm) irradiation according to the location and time, and incubation and counting, as shown in Fig. 3. For the control group, a dilution solution was distributed onto the TSA medium (0.3 mL with a micropipette) and uniformly applied with a disposable spreader. The medium was used rather than directly applying it to the surfaces of the shoe rack and toilet in the residential mock-up to prevent contamination with other background microorganisms. Although the disinfection performance against background microorganisms could have been assessed, this study focused on verifying the performance against *B. subtilis* (ATCC 6633). Additionally, direct application might have led to uneven microbial concentrations due to drying or evaporation, making it difficult to confirm the control case. Temperature and humidity were not specifically controlled but were monitored during the experiment to reflect the ambient conditions under which the tests were conducted.

Light in the UV wavelength region of 222 nm did not penetrate the plastic agar plate cover. A circular quartz plate was placed on the agar plate, considering damage such as dryness or falling of the microbial contaminant into the medium due to long-term irradiation. In general, the transmittance at 222 nm on a quartz plate is approximately 80 %. Measurements using a spectrometer confirmed that it was approximately 86 % (Fig. 4). Subsequently, the experiment was conducted by dividing the cases according to irradiation time, considering the distance between the lighting fixtures and the target within the mock-up site (Table 3).

The shoe rack (irradiance distance = 0.17 m) experiment was conducted three times for each case in Table 3, with varying irradiation times. The setup involved a general LED installed in the middle, below the 222 nm module at both ends, as shown in Fig. 5. The performances of the area under intense irradiation at 222 nm and the unexposed area

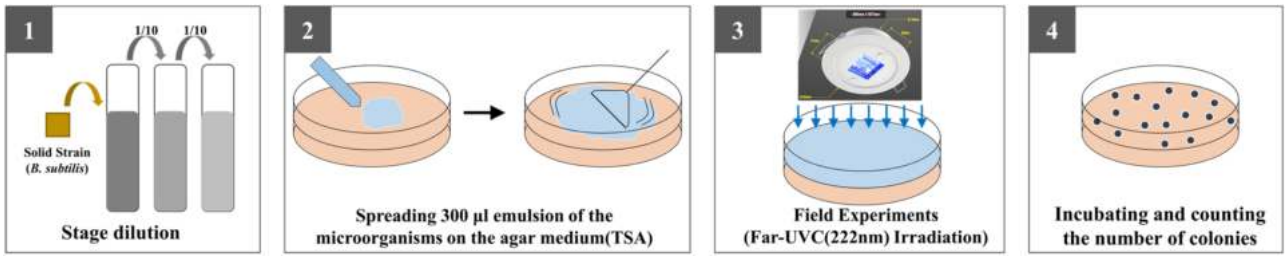

Fig. 3. Experiment process.

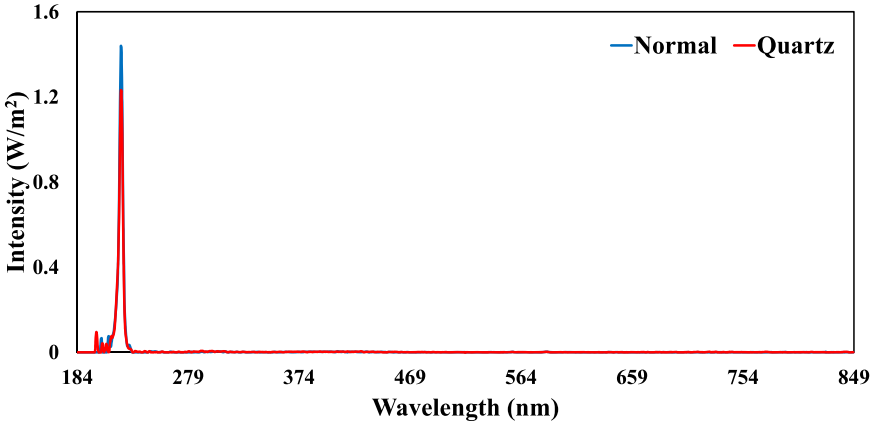

Fig. 4. Transmission performance of far-UVC (222 nm) module to quartz plate (normal case implies measurement without a quartz plate).

Table 3
Experiment cases by location and irradiation time (s).

	Shoe rack (distance = 0.17 m)	Toilet (distance = 1.8 m)
Case 0 (control)	0	
Case 1	60	3600
Case 2	120	7200
Case 3	180	10,800
Case 4	3000	14,400
Case 5	–	18,000

were compared. In addition, a short irradiation time was maintained, considering the sterilization coefficient of *B. subtilis* (ATCC 6633) at 222 nm [80]. L and R were below the 222 nm module of the shoe rack. C1 and C2 were below the general light.

The bathroom experiment primarily targeted the toilet surface (irradiance distance = 1.8 m), considering human hygiene activities. As shown in Fig. 6, the toilet experiment was simultaneously performed with the control experiment, with irradiation lasting up to 5 h at 1 h intervals. Three samples were tested every hour. As previously mentioned, the test certificate is based on the IEC standard for human safety received due to the use of an optical filter. However, the use of the optical filter can reduce the intensity, and the longer irradiation distance necessitated conducting the toilet case experiment twice.

2.5. Radiation analysis

A numerical analysis was conducted to evaluate the predicted values of disinfection performance. Bang et al. performed numerical analyses using UVC (254 nm) and compared the results between experiments and simulations [34]. Similarly, in the present study, a numerical analysis was conducted to compare the predicted values with experimental results for far-UVC (222 nm). Radiation analysis was performed using RADIANCE (Lawrence Berkeley National Laboratory, Berkeley, CA, USA), based on backward ray tracing and Monte Carlo algorithms. This analytical simulation, typically employed in lighting environments, such as lighting fixtures and solar analysis, calculates illuminance by considering complex diffusion, reflection, and transmission by combining R, G, and B channels [80]. By modeling the far-UVC excimer lamp module [81] used in the experiment, the intensity of the target surface was analyzed, assuming that the B channels were far-UVC (222 nm). However, considering the field experiment, the overall

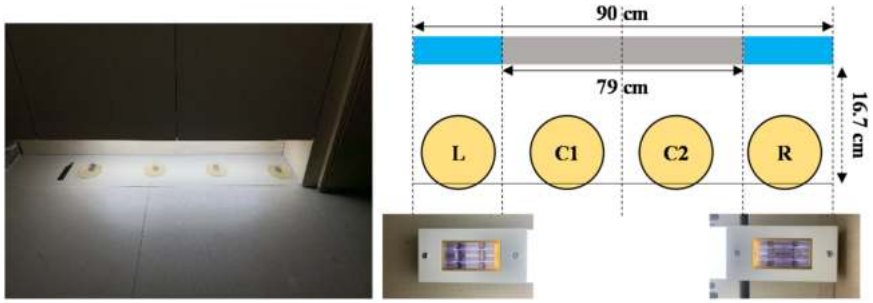

Fig. 5. 222 nm LED module on the shoe rack. (a) Measurement on the shoe rack. (b) Sampling location under a 222 nm bar-type module.

Fig. 6. 222 nm LED module on the bathroom. (a) Far-UVC module in the bathroom. (b) Measurement on the toilet.

implementation was impossible; therefore, only the intensity between the lamp and the target surface was calculated. The intensity of the target surface was calculated using RADIANCE software. The reduction rate based on the intensity calculated using Eq. (2) was predicted and compared with experimental results.

3. Results

3.1. Shoe rack reduction performance

The average temperature and humidity during the shoe rack experiment were 19.9 °C and 36.2 %, respectively. Table 4 presents the average *B. subtilis* (ATCC 6633) concentration according to the irradiation time and location. The *B. subtilis* concentration of the control case was 893 ± 40 CFU. C1 and C2, the areas under general LEDs, exhibited reduction rates of approximately 30–50 %. This was attributed to the influence of the 222 nm modules on both sides. L and R, the lower areas of the 222 nm modules, exhibited increased reduction rates over time. Moreover, the reduction rate was greater than 90 % after 5 min of irradiation. For the bar-type modules, the distance to the bottom surface and intensity measured using a spectrometer were approximately 17 cm and 54 μW/cm^2, respectively.

3.2. Bathroom reduction performance

The average temperature and humidity during the bathroom experiment were 17.5 °C and 29.3 %, respectively. The experimental results for the toilet were analyzed in two replicates, as presented in Table 5. The *B. subtilis* concentrations of the control cases were 780 ± 225 CFU. The reduction performance increased over time. Reduction rates of approximately 30 % and 62 % were observed after 3 and 5 h of irradiation, respectively. The distance from the ceiling to the toilet surface was approximately 1.8 m. Despite prolonged irradiation, achieving a 90 % reduction rate was challenging. The results are believed to be due to the influence of the reflection, diffusion, and obstruction of the 222-nm wavelength owing to the somewhat complex shapes of the fixtures in the bathroom, including the toilet, sink, and bathtub, as well as the conditions of the bathroom.

3.3. Sterilization coefficient, k

Based on the experimental results, the sterilization coefficient (k, cm^2/mJ) was obtained and compared with the dose-fraction survival rate, as shown in Fig. 7. The k values derived from the experimental results of the shoe rack (Fig. 7(a)) and bathroom (Fig. 7(b)) were 0.196 cm^2/mJ ($R^2 = 0.982$) and 0.202 cm^2/mJ ($R^2 = 0.811$), respectively. In addition, the k value derived from the reduction data for *B. subtilis* from the existing far-UVC (222 nm) data [81] was 0.1956 cm^2/mJ ($R^2 = 0.879$). This was calculated according to the single-stage decay in the UVGI handbook [23]. The shoe rack using the near-distance module and the bathroom using the relatively long-distance module exhibited results similar to the manufacturer's data.

The experimental results from the shoe rack showed minimal variation, and the k value derived from the dose-fraction curve exhibited high reliability. In the case of the bathroom, the presence of complex fixtures, such as the bathtub and sink, led to greater variation in the experimental results from repeated trials. However, the derived k value was an approximate value. This was consistent with the k value for UVC (254 nm), confirming that disinfection can be effectively achieved with the application of far-UVC (222 nm) in general residential spaces. Additionally, environmental factors, such as temperature and humidity, affect microbial disinfection performance when using UV lights [82–84]. In the present study, the shoe rack and bathroom experiments were performed in a full-scale residential building with similar temperature and humidity ranges; therefore, these environmental factors had no significant effect on the experimental results.

3.4. Evaluation of D_{90} (mJ/cm^2)

Based on the experimental results, the dose required to achieve the target reduction rate was calculated using Eq. (3). This metric is expressed in various forms, such as sterilization and disinfection rates, and can be compared using D_{90}, D_{99}, and $D_{99.9}$. Table 6 presents the calculation and comparison of D_{90} [53,58,59,65]. We calculated the D_{90} values using the manufacturer's k value for *B. subtilis*, and the experimental results were nearly identical to those of the shoe rack irradiated with far-UVC (222 nm) at a relatively short distance. The down-light type used in the bathroom was expected to achieve 90 % disinfection with a dose lower than the standard value. However, the high-humidity environment in the bathroom, where water is frequently used, may favor microbial growth. Therefore, rather than relying solely on the D_{90} value for comparison, it may be necessary to establish a more reliable method for determining the appropriate dose.

3.5. Prediction for disinfection performance

The time required to achieve the desired reduction rate can be estimated based on the intensity predicted using RADIANCE and the k derived from the experiment [34]. Modeling and radiation analysis for the shoe rack were performed owing to the challenges associated with the actual modeling of the bathroom, as shown in Figs. 5 and 8. The intensity was concentrated under the L and R points where the 222 nm module was installed, and the reflectance of the wall and floor was applied to the shoe rack. The far-UVC (222 nm) intensities were 0.167 and 0.17 mW/cm^2 at the L and R points ($x \pm 0.395$ m, y 0 m, $z - 0.167$ m), respectively.

To compare with the previously estimated D_{90}, the time required for a 90 % reduction was calculated and is presented in Table 7. Radiation analysis indicated that a 90 % reduction could be achieved within approximately 69 s. In addition, a 90 % reduction time was predicted to be achieved within approximately 64 s based on the actual measured intensity value. However, an actual experiment with irradiation time revealed that a 90 % reduction in performance was achieved with approximately 5 min of irradiation.

The evaluation of disinfection performance using radiation analysis presented herein showed results similar to those of experiments using the k values. This approach appears to be appropriate for residential spaces. However, there were some discrepancies with the actual experimental results. These differences could be attributed to factors such as the use of a medium and quartz plate, the general LED section of the lighting applied to the shoe rack, and the environmental characteristics of the target area (e.g., temperature, humidity, and moisture content). This suggests that relying solely on equipment specifications to evaluate and predict disinfection performance may be insufficient.

More accurate performance prediction and evaluation could be achieved by considering relevant environmental factors, such as the

Table 4
Number of surface *B. subtilis* colonies in shoe rack (values are the averages obtained by sampling three times).

	Non-far-UVC		Far-UVC	
Control Case				
CFU/mL	893 ± 40			
Case 1 60 s				
CFU/mL	620 ± 71		515 ± 124	
Case 2 120 s				
CFU/mL	563 ± 158		262 ± 92	
Case 3 180 s				
CFU/mL	633 ± 56		186 ± 53	
Case 4 300 s				
CFU/mL	511 ± 49		79 ± 76	

scale and reflectance of the target area. Additionally, immediate reduction is crucial in scenarios involving infectious bacteria. Therefore, accurate performance evaluations should reflect the specific characteristics of the actual space intended for application.

4. Discussion

The k values derived from the experiments were relatively consistent. Most previous studies evaluated the reduction performance of microorganisms by examining the far-UVC within a close range. In our study, the shoe rack experiment, conducted at a shorter distance, demonstrated effectiveness within a relatively short irradiation time. However, despite using the same k value, the bathroom required longer irradiation times due to the reduced intensity caused by the greater distance. Although the k value itself did not change significantly, the increase in distance necessitated longer irradiation times, indicating that designing far-UVC systems solely based on the module's performance may be inappropriate. Relying only on equipment specifications is insufficient to predict effectiveness through dose calculations. Therefore, it is necessary to estimate the intensity of the lighting equipment and predict the reduction performance according to relevant variables such as indoor conditions (airflow, temperature, and humidity) and distance [79–81]. Additionally, long-term irradiation requires an evaluation of the indicators and improvement strategies. Given that the

Table 5
Number of surface *B. subtilis* colonies in bathroom (values are the averages obtained by sampling six times).

Control Case			
CFU/mL	780 ± 225		
Case 1 1 h			
CFU/mL	690 ± 242		
Case 2 2 h			
CFU/mL	640 ± 323		
Case 3 3 h			
CFU/mL	550 ± 365		
Case 4 4 h			
CFU/mL	386 ± 275		
Case 5 5 h			
CFU/mL	291 ± 177		

duration of irradiation is a time-based parameter, it is crucial to confirm whether the observed reduction is due to the 222 nm wavelength or is simply a result of time.

Prolonged irradiation times have proven effective in residential spaces, and this method is deemed safe based on the IEC certification. Most studies on microbial disinfection and sterilization at 222 nm have demonstrated the effectiveness of this approach [57,60,62,63]. Furthermore, field applications have shown that greater distances require extended irradiation times. Although Xie et al. [66] included elevator-scale targets, when applying this method to residential spaces, additional environmental factors and conditions must be considered, such as changes in temperature and humidity within the living space due to real-life activities (e.g., cooking, showering, and resting). These considerations are crucial to effectively address infectious diseases and microbial contamination in residential environments.

Previous studies have confirmed the effects of far-UVC on microbial reduction. In this study, *B. subtilis* (ATCC 6633), a nonpathogenic bacterium, was tested. The use of far-UVC is considered an appropriate

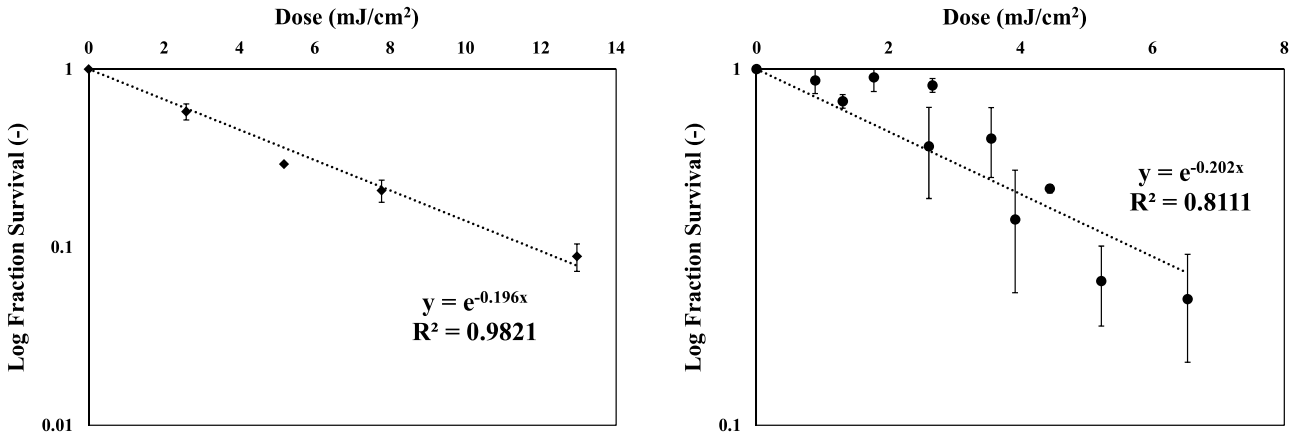

Fig. 7. *Bacillus subtilis* inactivation curves by case. (a) Shoe rack and (b) bathroom.

Table 6
D_{90} value by case.

	Standard*	Shoe rack	Bathroom
k (cm²/mJ)	0.1956	0.196	0.202
D_{90} (mJ/cm²)	11.77	11.75	11.4

* Standard indicated the manufacturer data [81].

preventive measure against microbial contamination in residential spaces. Besides, the reduction in SARS-CoV-2 and H1N1, as presented in a previous study [59], demonstrated its high potential as a countermeasure against infectious diseases. The k values for SARS-CoV-2 and influenza A (H1N1) were larger than those for *Bacillus*; therefore, a faster reduction was expected [59].

This study focused on surface microorganisms. However, indoor airborne microorganisms may produce different results depending on the type of microorganism or infectious bacteria. In addition, the influencing factors may vary. Far-UVC has application principles similar to those of UV-C; therefore, many research techniques, such as CFD analysis [85], fluence rate, distribution, and performance prediction, can be employed. Safety should be prioritized when using far-UVCs in a residential space. However, achieving an appropriate reduction performance requires an increased output through the combination and development of far-UVCs.

The findings of this study demonstrate the suitability of far-UVC (222 nm) for residential spaces. A reduction performance exceeding 90 % can be expected even with small doses. However, achieving optimal disinfection performance requires long durations and the distance to the target must also be considered. This can be analyzed in terms of energy consumption. Nonetheless, further development is needed in several areas to ensure adequate reduction in performance and energy use. Additionally, far-UVC (222 nm) has the potential to generate ozone [86, 87], which necessitates additional consideration for its application in residential spaces with limited ventilation. Therefore, it is essential to develop safer and more effective methods, such as combining dimming systems based on human detection and operational scheduling according to occupancy patterns.

Few studies have explored the application of 222 nm far-UVC in residential settings, particularly in high-contact areas where both safety and efficacy are essential. Our findings provide foundational data on the disinfection performance of far-UVC at varying distances and exposure times, establishing a benchmark for future research in similar environments. Overall, our results suggest that implementing far-UVC technology in household settings can significantly reduce microbial contamination on frequently contacted surfaces, such as those in bathrooms and on shoe racks, offering valuable guidance for enhancing hygiene management in residential spaces. The observed efficacy of 222 nm far-UVC at safe exposure levels further supports its potential as an

Table 7
Comparison between the disinfection time for a 90 % reduction performance according to prediction and the shoe rack experiment.

	Measurement	Prediction (RADIANCE)
Intensity (mW/cm²)	0.184	Average L, R 0.17
Required time for 90 % reduction	63.8 s	69.1 s

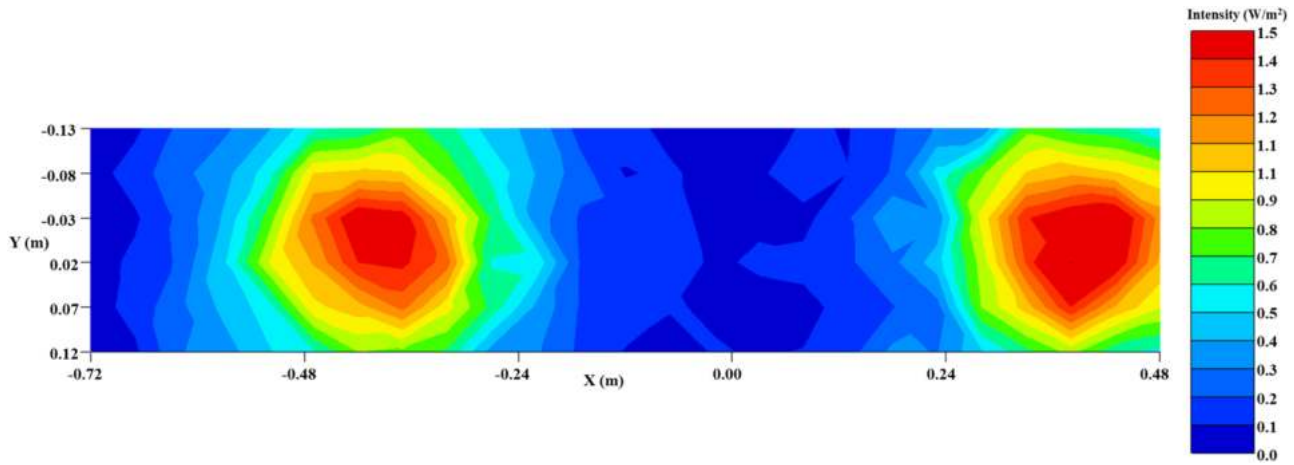

Fig. 8. Radiation analysis using RADIANCE for the far-UVC module on the shoe rack.

alternative to traditional 254 nm UV-C for residential disinfection, thus expanding the theoretical understanding of disinfection kinetics and the practical effectiveness of safer UVC wavelengths. The *k* values and reduction rates identified in this study for *B. subtilis* can also serve as baseline data for future studies investigating far-UVC efficacy across various residential settings and microbial targets.

Furthermore, future research could benefit from utilizing machine learning approaches [88–90] to optimize the practical implementation of far-UVC disinfection systems. By training predictive models on data such as *k* values, microbial reduction rates, and environmental factors (e.g., temperature, humidity, and distance), machine learning could enhance the predictive accuracy of disinfection efficacy across diverse residential conditions. Such models could also help analyze correlations between various environmental factors and disinfection performance, ultimately guiding the design of more effective far-UVC systems in occupied spaces.

5. Conclusions

This study demonstrates the potential of 222 nm far-UVC as an effective and safe disinfection solution for residential environments. Our experiments showed a significant reduction in microbial contamination on high-contact surfaces, such as shoe racks and bathrooms, under controlled conditions. These findings contribute to the theoretical understanding of far-UVC efficacy by establishing a practical baseline for microbial reduction rates at varying distances and irradiation times, expanding UV disinfection research beyond traditional commercial and healthcare settings.

Our results also suggest that 222 nm far-UVC might serve as a practical tool for reducing microbial contamination in home environments. Its application could lead to significant improvements in household hygiene, particularly in areas with frequent human contact. To achieve optimal performance, however, far-UVC systems should be calibrated to account for environmental variables, such as distance, intensity, and surface reflectivity, which directly influence disinfection efficacy.

Despite these promising findings, this study has certain limitations. Although the use of *B. subtilis* as a test organism provides a conservative model, further studies involving other microorganisms, including viruses, would help to generalize the results. Additionally, practical applications should address potential challenges, such as ozone generation and energy consumption associated with prolonged far-UVC use. By addressing these challenges, far-UVC technology could be developed into a valuable component of future household hygiene management.

Funding

This research was supported by the National Research Foundation of Korea (NRF) grant, funded by the Korean government (MSIT; grant no. RS-2023–00209080).

CRediT authorship contribution statement

Jong-Il Bang: Writing – review & editing, Writing – original draft, Visualization, Validation, Software, Methodology, Investigation, Data curation. **Ye-Lim Jo:** Resources, Investigation, Data curation. **Eun-Tack Lee:** Resources, Project administration, Funding acquisition. **Minki Sung:** Supervision, Funding acquisition, Conceptualization.

Declaration of competing interest

The authors declare that they have no known competing financial interests or personal relationships that could have appeared to influence the work reported in this paper.

Data availability

Data will be made available on request.

References

[1] World Health Organization, WHO COVID-19 dashboard. http://covid19.who.int/. (accessed 5 October 2023).
[2] World Health Organization, Coronavirus disease (COVID-19). http://who.int/health-topics/coronavirus. (accessed 5 October 2023).
[3] Korea Disease Control and Prevention Agency, The 2015 MERS outbreak in the Republic of Korea: learning from MERS, KMOHW (2016).
[4] World Health Organization, Getting your workplace ready for COVID-19, 2020. https://www.who.int/docs/default-source/coronaviruse/getting-workplace-ready-for-covid-19.pdf. (accessed 18 March 2024).
[5] Center for systems science and engineering (CSSE) at Johns hopkins university (JHU), COVID-19 Dashboard (2023). http://coronavirus.jhu.edu/map.html (accessed 5 October 2023).
[6] M. Ki, 2015 MERS outbreak in Korea: hospital-to-hospital transmission, Epidemiol. Health. 37 (2015) e2015033, https://doi.org/10.4178/epih/e2015033.
[7] K.S. Kwon, J.I. Park, Y.J. Park, D.M. Jung, K.W. Ryu, J.H. Lee, Evidence of long-distance droplet transmission of SARS-CoV-2 by direct air flow in a restaurant in Korea, J. Korean Med. Sci. 35 (2020) e415, https://doi.org/10.3346/jkms.2020.35.e415.
[8] S.E. Hwang, J.H. Chang, B. Oh, J. Heo, Possible aerosol transmission of COVID-19 associated with an outbreak in an apartment in Seoul, South Korea, 2020, Int. J. Infect. Dis. 104 (2021) 73–76, https://doi.org/10.1016/j.ijid.2020.12.035.
[9] I.T.S. Yu, Y. Li, T.W. Wong, W. Tam, A.T. Chan, J.H.W. Lee, D.Y.C. Leung, T. Ho, Evidence of airborne transmission of the severe acute respiratory syndrome virus, N. Engl. J. Med. 350 (2004) 1731–1739, https://doi.org/10.1056/NEJMoa032867.
[10] K.R. McKinney, Y.Y. Gong, T.G. Lewis, Environmental transmission of SARS at Amoy Gardens, J. Environ. Health. 68 (2006) 26–30, quiz 51.
[11] J. Lu, J. Gu, K. Li, C. Xu, W. Su, Z. Lai, D. Zhou, C. Yu, B. Xu, Z. Yang, COVID-19 outbreak associated with air conditioning in restaurant, Guangzhou, China, 2020, Emerg. Infect. Dis. 26 (2020) 1628–1631, https://doi.org/10.3201/eid2607.200764.
[12] Y. Li, H. Qian, J. Hang, X. Chen, L. Hong, P. Liang, J. Li, S. Xiao, J. Wei, L. Liu, M. Kang, Evidence for probable aerosol transmission of SARS-CoV-2 in a poorly ventilated restaurant, MedRxiv. Published online April 22 (2020), https://doi.org/10.1101/2020.04.16.20067728.
[13] M. Kang, J. Wei, J. Yuan, J. Guo, Y. Zhang, J. Hang, Y. Qu, H. Qian, Y. Zhuang, X. Chen, X. Peng, T. Shi, J. Wang, J. Wu, T. Song, J. He, Y. Li, N. Zhong, Probable evidence of fecal aerosol transmission of SARS-CoV-2 in a high-rise building, Ann. Intern. Med. 173 (2020) 974–980, https://doi.org/10.7326/M20-0928.
[14] H. Qian, T. Miao, L. Liu, X. Zheng, D. Luo, Y. Li, Indoor transmission of SARS-CoV-2, Indoor, Air 31 (2021) 639–645, https://doi.org/10.1111/ina.12766.
[15] EPA, United States environmental protection agency, a brief guide to mold, moisture and your home. https://www.epa.gov/mold/brief-guide-mold-moisture-and-your-home. (accessed 5 October 2023).
[16] S.N.H.D. Public, Accommodation Facilities Regulation: Mold Remediation Guidelines, South Nevada Health District, 2006.
[17] EPA, Moisture control guidance for building design, constructions and maintenance, 2013. https://www.epa.gov/sites/default/files/2014-08/documents/moisture-control.pdf. (accessed 25 March 2024).
[18] EPA, Mold remediation in schools and commercial buildings, 2008. https://www.epa.gov/mold/printable-version-mold-remediation-schools-and-commercial-buildings. (accessed 25 March 2024).
[19] EPA, Guidelines on assessment and remediation of fungi in indoor environments, 2008. https://home.nyc.gov/assets/doh/downloads/pdf/epi/epi-mold-guidelines.pdf. (accessed 25 March 2024).
[20] WHO, WHO guidelines for indoor air quality – Dampness and mould, 2009. https://www.who.int/publications/i/item/9789289041683. (accessed 25 March 2024).
[21] EPA, A brief guide to mold moisture and your home, 2010. https://www.epa.gov/mold/brief-guide-mold-moisture-and-your-home. (accessed 25 March 2024).
[22] IESO/ASHRAE, 3210, Standard guide for the assessment of education facilities for moisture affected areas and fungal contamination, 2014. http://mtpinnacle.com/pdfs/bsr-ashrae-iaqa%203210p_2ndpprdraft.pdf. (accessed 25 March 2024).
[23] W. Kowalski, Ultraviolet Germicidal Irradiation Handbook, Springer, New York, 2009, https://doi.org/10.1007/978-3-642-01999-9.
[24] Ultraviolet Air and Surface Treatment, ASHRAE Handbook-HVAC Application, ASHRAE, Oak Ridge, 2019.
[25] ISO 15727:2020, UV-C devices-measurement of the output of a UV-C lamp.
[26] ISO 15714:2019, method of evaluating the UV dose to airborne microorganisms transiting in-duct ultraviolet germicidal irradiation devices.
[27] ISO 15858:2020, UV-C devices-safety information-permissible human exposure.
[28] O. Strindehag, I. Josefsson, E. Henningson, Emission of bacteria from air humidifiers, Environ. Int. 17 (1991) 235–241, https://doi.org/10.1016/0160-4120(91)90008-E.
[29] E. Levetin, R. Shaughnessy, C.A. Rogers, R. Scheir, Effectiveness of germicidal UV radiation for reducing fungal contamination within air-handling units, Appl. Environ. Microbiol. 67 (2001) 3712–3715, https://doi.org/10.1128/AEM.67.8.3712-3715.2001.

[30] D. Menzies, J. Popa, J.A. Hanley, T. Rand, D.K. Milton, Effect of ultraviolet germicidal lights installed in office ventilation systems on workers' health and wellbeing: double-blind multiple crossover trial, Lancet 362 (2003) 1785–1791, https://doi.org/10.1016/S0140-6736(03)14897-0.
[31] E. Kujundzic, M. Hernandez, S.L. Miller, Ultraviolet germicidal irradiation inactivation of airborne fungal spores and bacteria in upper-room air and HVAC in-duct configurations, J. Environ. Eng. Sci. 6 (2007) 1–9, https://doi.org/10.1139/s06-039.
[32] J. Lau, W. Bahnfleth, J. Freihaut, Estimating the effects of ambient conditions on the performance of UVGI air cleaners, Build. Environ. 44 (2009) 1362–1370, https://doi.org/10.1016/j.buildenv.2008.05.015.
[33] Y. Yang, H. Zhang, V. Chan, A.C. Lai, Development and experimental validation of a mathematical model for the irradiance of in-duct ultraviolet germicidal lamps, Build. Environ. 152 (2019) 160–171, https://doi.org/10.1016/j.buildenv.2019.02.004.
[34] J.I. Bang, J.Y. Park, Y.L. Jo, J.W. Jeong, A. Choi, M. Sung, Sterilization effectiveness of in-duct ultraviolet germicidal irradiation system in liquid desiccant and indirect/direct evaporative cooling-assisted 100% outdoor air system, Build. Environ. 186 (2020) 107350, https://doi.org/10.1016/j.buildenv.2020.107350.
[35] W.J. Kowalski, W.P. Bahnfleth, J.L. Rosenberger, Dimensional analysis of UVGI air disinfection systems, HVAC R Res 9 (2003) 347–363, https://doi.org/10.1080/10789669.2003.10391074.
[36] F. Atci, Y.E. Cetin, M. Avci, O. Aydin, Evaluation of in-duct UV-C lamp array on air disinfection: a numerical analysis, Sci. Technol. Built Environ. 27 (2021) 98–108, https://doi.org/10.1080/23744731.2020.1776549.
[37] P. Xu, J. Peccia, P. Fabian, J.W. Martyny, K.P. Fennelly, M. Hernandez, S.L. Miller, Efficacy of ultraviolet germicidal irradiation of upper-room air in inactivating airborne bacterial spores and mycobacteria in full-scale studies, Atmos. Environ. 37 (2003) 405–419, https://doi.org/10.1016/S1352-2310(02)00825-7.
[38] A. Hollaender, J.W. Oliphant, The inactivating effect of monochromatic ultraviolet radiation on influenza virus, J. Bacteriol. 48 (1944) 447–454, https://doi.org/10.1128/jb.48.4.447-454.1944.
[39] J.M. Macher, L.E. Alevantis, Y.L. Chang, K.S. Liu, Effect of ultraviolet germicidal lamps on airborne microorganisms in an outpatient waiting room, Appl. Occup. Environ. Hyg. 7 (1992) 505–513, https://doi.org/10.1080/1047322X.1992.10390201.
[40] G. Ko, M.W. First, H.A. Burge, The characterization of upper-room ultraviolet germicidal irradiation in inactivating airborne microorganisms, Environ. Health Perspect. 110 (2002) 95–101, https://doi.org/10.1289/ehp.0211095.
[41] A.C.K. Lai, S.S. Nunayon, A new UVC-LED system for disinfection of pathogens generated by toilet flushing, Indoor, Air 31 (2021) 324–334, https://doi.org/10.1111/ina.12752.
[42] S.S. Nunayon, H. Zhang, A.C.K. Lai, Comparison of disinfection performance of UVC-LED and conventional upper-room UVGI systems, Indoor, Air 30 (2020) 180–191, https://doi.org/10.1111/ina.12619.
[43] S.S. Nunayon, H.H. Zhang, A.C.K. Lai, A novel upper-room UVC-LED irradiation system for disinfection of indoor bioaerosols under different operating and airflow conditions, J. Hazard. Mater. 396 (2020) 122715, https://doi.org/10.1016/j.jhazmat.2020.122715.
[44] D.K. Kim, D.H. Kang, UVC LED irradiation effectively inactivates aerosolized viruses, bacteria, and fungi in a chamber-type air disinfection system, Appl. Environ. Microbiol. 84 (2018), https://doi.org/10.1128/AEM.00944-18 e00944-18.
[45] J.I. Bang, J. Park, A. Choi, J.W. Jeong, J.Y. Kim, M. Sung, Evaluation of UR-UVGI system for sterilization effect on microorganism contamination in negative pressure isolation ward, Sustainability 10 (2018) 3192, https://doi.org/10.3390/su10093192.
[46] C.J. Noakes, P.A. Sleigh, L.A. Fletcher, C.B. Beggs, Use of CFD modelling to optimise the design of upper-room UVGI disinfection systems for ventilated rooms, Indoor Built Environ 15 (2006) 347–356, https://doi.org/10.1177/1420326X06067353.
[47] C.J. Noakes, C.B. Beggs, P.A. Sleigh, Modelling the performance of upper room ultraviolet germicidal irradiation devices in ventilated rooms: comparison of analytical and CFD methods,https://www.editorialmanager.com/rineng/default.aspx, Indoor Built Environ 13 (2004) 477–488, https://doi.org/10.1177/1420326X04049343.
[48] M. Sung, S. Kato, Method to evaluate UV dose of upper-room UVGI system using the concept of ventilation efficiency, Build. Environ. 45 (2010) 1626–1631, https://doi.org/10.1016/j.buildenv.2010.01.011.
[49] M. Sung, S. Kato, Estimating the germicidal effect of upper-room UVGI system on exhaled air of patients based on ventilation efficiency, Build. Environ. 46 (2011) 2326–2332, https://doi.org/10.1016/j.buildenv.2011.05.015.
[50] C.A. Gilkeson, C. Noakes, Application of CFD simulation to predicting upper-room UVGI effectiveness, Photochem. Photobiol. 89 (2013) 799–810, https://doi.org/10.1111/php.12013.
[51] C.A. Gilkeson, C.J. Noakes, M.A.I. Khan, Computational fluid dynamics modelling and optimisation of an upper-room ultraviolet germicidal irradiation system in a naturally ventilated hospital ward, Indoor Built Environ 23 (2014) 449–466, https://doi.org/10.1177/1420326X14532933.
[52] M. Kanaan, N. Ghaddar, K. Ghali, G. Araj, New airborne pathogen transport model for upper-room UVGI spaces conditioned by chilled ceiling and mixed displacement ventilation: enhancing air quality and energy performance, Energy Convers. Manag. 85 (2014) 50–61, https://doi.org/10.1016/j.enconman.2014.05.073.
[53] M. Buonanno, G. Randers-Pehrson, A.W. Bigelow, S. Trivedi, F.D. Lowy, H. M. Spotnitz, S.M. Hammer, D.J. Brenner, 207-nm UV light-a promising tool for safe low-cost reduction of surgical site infections. I: in vitro studies, PLOS ONE 8 (2013) e76968, https://doi.org/10.1371/journal.pone.0076968.
[54] M. Buonanno, M. Stanislauskas, B. Ponnaiya, A.W. Bigelow, G. Randers-Pehrson, Y. Xu, I. Shuryak, L. Smilenov, D.M. Owens, D.J. Brenner, 207-nm UV light—A promising tool for safe low-cost reduction of surgical site infections. II: in-vivo safety studies, PLOS ONE 11 (2016) e0138418, https://doi.org/10.1371/journal.pone.0138418.
[55] M. Buonanno, B. Ponnaiya, D. Welch, M. Stanislauskas, G. Randers-Pehrson, L. Smilenov, F.D. Lowy, D.M. Owens, D.J. Brenner, Germicidal efficacy and mammalian skin safety of 222-nm UV light, Radiat. Res. 187 (2017) 483–491, https://doi.org/10.1667/RR0010CC.1.
[56] K. Narita, K. Asano, Y. Morimoto, T. Igarashi, A. Nakane, Chronic irradiation with 222-nm UVC light induces neither DNA damage nor epidermal lesions in mouse skin, even at high doses, PLOS ONE 13 (2018) e0201259, https://doi.org/10.1371/journal.pone.0201259.
[57] K. Narita, K. Asano, Y. Morimoto, T. Igarashi, M.R. Hamblin, T. Dai, A. Nakane, Disinfection and healing effects of 222-nm UVC light on methicillin-resistant staphylococcus aureus infection in mouse wounds, J. Photochem. Photobiol. B. 178 (2018) 10–18, https://doi.org/10.1016/j.jphotobiol.2017.10.030.
[58] D. Welch, M. Buonanno, V. Grilj, I. Shuryak, C. Crickmore, A.W. Bigelow, G. Randers-Pehrson, G.W. Johnson, D.J. Brenner, Far-UVC light: a new tool to control the spread of airborne-mediated microbial diseases, Sci. Rep. 8 (2018) 2752, https://doi.org/10.1038/s41598-018-21058-w.
[59] M. Buonanno, D. Welch, I. Shuryak, D.J. Brenner, Far-UVC light (222 nm) efficiently and safely inactivates airborne human coronaviruses, Sci. Rep. 10 (2020) 10285, https://doi.org/10.1038/s41598-020-67211-2.
[60] N. Yamano, M. Kunisada, S. Kaidzu, K. Sugihara, A. Nishiaki-Sawada, H. Ohashi, A. Yoshioka, T. Igarashi, A. Ohira, M. Tanito, C. Nishigori, Long-term effects of 222-nm ultraviolet radiation C sterilizing lamps on mice susceptible to ultraviolet radiation, Photochem. Photobiol. 96 (2020) 853–862, https://doi.org/10.1111/php.13269.
[61] W. Taylor, E. Camilleri, D.L. Craft, G. Korza, M.R. Granados, J. Peterson, R. Szczpaniak, S.K. Weller, R. Moeller, T. Douki, W.W.K. Mok, P. Setlow, DNA Damage Kills Bacterial Spores and Cells Exposed to 222-Nanometer UV Radiation, Appl. Environ. Microbiol. 86 (2020), https://doi.org/10.1128/AEM.03039-19 e03039-19.
[62] H. Kitagawa, T. Nomura, T. Nazmul, K. Omori, N. Shigemoto, T. Sakaguchi, H. Ohge, Effectiveness of 222-nm ultraviolet light on disinfecting SARS-CoV-2 surface contamination, Am. J. Infect. Control. 49 (2021) 299–301, https://doi.org/10.1016/j.ajic.2020.08.022.
[63] J.I. Bang, J.H. Kim, A. Choi, M. Sung, The wavelength-based inactivation effects of a light-emitting diode module on indoor microorganisms, Int. J. Environ. Res. Public Health. 19 (2022) 9659, https://doi.org/10.3390/ijerph19159659.
[64] E. Eadie, W. Hiwar, L. Fletcher, E. Tidswell, P. O'Mahoney, M. Buonanno, D. Welch, C.S. Adamson, D.J. Brenner, C. Noakes, K. Wood, U.V.C. Far, Far-UVC (222 nm) efficiently inactivates an airborne pathogen in a room-sized chamber, Sci. Rep. 12 (2022) 4373, https://doi.org/10.1038/s41598-022-08462-z.
[65] R.T. Robinson, N. Mahfooz, O. Rosas-Mejia, Y. Liu, N.M. Hull, UV222 disinfection of SARS-CoV-2 in solution, Sci. Rep. 12 (2022) 14545, https://doi.org/10.1038/s41598-022-18385-4.
[66] R. Xie, G.Y. Tse, L.C. Man, A.L. Cheung, D.T. Wong, E.H. Lam, H. Huang, D. Y. Leung, Systematical investigations on disinfection effectiveness of Far-UVC (222 nm) irradiation: from laboratory study to field tests, J. Appl. Environ. Microbiol. 10 (2022) 17–34, https://doi.org/10.12691/jaem-10-1-3.
[67] W.L. Nicholson, N. Munakata, G. Horneck, H.J. Melosh, P. Setlow, Resistance of Bacillus endospores to extreme terrestrial and extraterrestrial environments, Microbiol. Mol. Biol. Rev. 64 (2000) 548–572, https://doi.org/10.1128/MMBR.64.3.548-572.2000.
[68] F. Mostafazadeh, F. Kilanehei, M. Hassanlourad, Experimental investigation of contaminant transport through saturated porous media under groundwater flow, Amirkabir J. Civ. Eng. 52 (2020) 89–106.
[69] F. Mostafazadeh, F. Kilanehei, M. Hassanlourad, Experimental evaluation of self-remediation mechanism by groundwater flow in unconfined aquifers, Water Environ. Res. 93 (2021) 1005–1018, https://doi.org/10.1002/wer.1489.
[70] M.A. Abdelzaher, E.M. Farahat, H.M. Abdel-Ghafar, B.A.A. Balboul, M.M. Awad, Environmental policy to develop a conceptual design for the water-energy-food Nexus: a case study in Wadi-Dara on the Red Sea Coast, Egypt, Water 15 (2023) 780, https://doi.org/10.3390/w15040780.
[71] M.A. Abdelzaher, A.S. Hamouda, I.M. El-Kattan, A comprehensive study on the fire resistance properties of ultra-fine ceramic waste-filled high alkaline white cement paste composites for progressing towards sustainability, Sci. Rep. 13 (2023) 22097, https://doi.org/10.1038/s41598-023-49229-4.
[72] M.A. Abdelzaher, Sustainable development goals for industry, innovation, and infrastructure: demolition waste incorporated with nanoplastic waste enhanced the physicomechanical properties of white cement paste composites, Appl. Nanosci. 13 (2023) 1–16, https://doi.org/10.1007/s13204-023-02766-w.
[73] R. Abbas, M.A. Abdelzaher, N. Shehata, M.A. Tantawy, Production, characterization and performance of green geopolymer modified with industrial by-products, Sci. Rep. 14 (2024) 5104, https://doi.org/10.1038/s41598-024-55494-8.
[74] M.A. Abdelzaher, A.S. Hamouda, I.M. Ismail, M.A. El-Sheikh, Nanotitania reinforced limestone cement: physico-mechanical investigation, Key Eng. Mater. 786 (2018) 248–257, https://doi.org/10.4028/www.scientific.net/KEM.786.248.
[75] V. Richard, P. Van der Auwera, R. Snoeck, D. Daneau, F. Meunier, Nosocomial bacteremia caused by *Bacillus* species, Eur. J. Clin. Microbiol. Infect. Dis. 7 (1988) 783–785, https://doi.org/10.1007/BF01975049.

[76] A.S. de Boer, B. Diderichsen, On the safety of *Bacillus subtilis* and *B. amyloliquefaciens*: a review, Appl. Microbiol. Biotechnol. 36 (1991) 1–4, https://doi.org/10.1007/BF00164689.
[77] M.R. Oggioni, G. Pozzi, P.E. Valensin, P. Galieni, C. Bigazzi, Recurrent septicemia in an immunocompromised patient due to probiotic strains of *Bacillus subtilis*, J. Clin. Microbiol. 36 (1998) 325–326, https://doi.org/10.1128/JCM.36.1.325-326.1998.
[78] W.L. Nicholson, B. Galeano, UV resistance of Bacillus anthracis spores revisited: validation of Bacillus subtilis spores as UV surrogates for spores of B. anthracis Sterne, Appl. Environ. Microbiol. 69 (2003) 1327–1330, https://doi.org/10.1128/AEM.69.2.1327-1330.2003.
[79] ISO 16000-17:2011, indoor air-part 17: detection and enumeration of moulds-culture-based method.
[80] G. Ward, R.A. Shakespeare, Rendering With Radiance: The Art and Science of Lighting Visualization, Morgan Kaufmann Publishers, Michigan, 1998.
[81] https://www.ushio.com/(accessed 5 October 2023), Care222® Filtered Far UV-C Excimer Lamp Module, USHIO America, Inc., 2023. https://www.ushio.eu/wp-content/uploads/2022/02/UAI_FLYER_care222-filtered-far-uv-c-excimer-lamp-module.pdf.
[82] P. Xu, E. Kujundzic, J. Peccia, M.P. Schafer, G. Moss, M. Hernandez, S.L. Miller, Impact of environmental factors on efficacy of upper-room air ultraviolet germicidal irradiation for inactivating airborne mycobacteria, Environ. Sci. Technol. 39 (2005) 9656–9664, https://doi.org/10.1021/es0504892.
[83] G. Berry, A. Parsons, M. Morgan, J. Rickert, H. Cho, A review of methods to reduce the probability of the airborne spread of COVID-19 in ventilation systems and enclosed spaces, Environ. Res. 203 (2022) 111765, https://doi.org/10.1016/j.envres.2021.111765.
[84] Y. Qiao, M. Yang, I.A. Marabella, D.A.J. McGee, H. Aboubakr, S. Goyal, C. J. Hogan Jr., B.A. Olson, M. Torremorell, Greater than 3-log reduction in viable coronavirus aerosol concentration in ducted ultraviolet-C (UV–C) systems, Environ. Sci. Technol. 55 (2021) 4174–4182, https://doi.org/10.1021/acs.est.0c05763.
[85] A.G. Buchan, L. Yang, D. Welch, D.J. Brenner, K.D. Atkinson, Improved estimates of 222 nm far-UVC susceptibility for aerosolized human coronavirus via a validated high-fidelity coupled radiation-CFD code, Sci. Rep. 11 (2021) 19930, https://doi.org/10.1038/s41598-021-99204-0.
[86] Z. Peng, D.A.J. Day, G.A. Symonds, O.J. Jenks, H. Stark, A.V. Handschy, J.A. de Gouw, J.L. Jimenez, Significant production of ozone from germicidal UV lights at 222 nm, Environ. Sci. Technol. Lett. 10 (2023) 668–674, https://doi.org/10.1021/acs.estlett.3c00314.
[87] M.F. Link, A. Shore, B.H. Hamadani, D. Poppendieck, Ozone generation from a germicidal ultraviolet lamp with peak emission at 222 nm, Environ. Sci. Technol. Lett. 10 (2023) 675–679, https://doi.org/10.1021/acs.estlett.3c00318.
[88] A. Akbarpour, M. Mahdikhani, R.Ziaie Moayed, Mechanical behavior and permeability of plastic concrete containing natural zeolite under triaxial and uniaxial compression, J. Mater. Civ. Eng. 34 (2022) 04021453, https://doi.org/10.1061/(ASCE)MT.1943-5533.0004093.
[89] A. Akbarpour, M. Mahdikhani, Effects of natural zeolite and sulfate environment on mechanical properties and permeability of cement-bentonite cutoff wall, Eur. J. Environ. Civ. Eng. 27 (2023) 1165–1178, https://doi.org/10.1080/19648189.2022.2075940.
[90] S.F. Fazel Mojtahedi, A. Akbarpour, A.G. Darzi, H. Sadeghi, M.T. van Genuchten, Prediction of stress-dependent Soil water Retention using machine learning, Geotech. Geol. Eng. 42 (2024) 3939–3966, https://doi.org/10.1007/s10706-024-02767-8.